

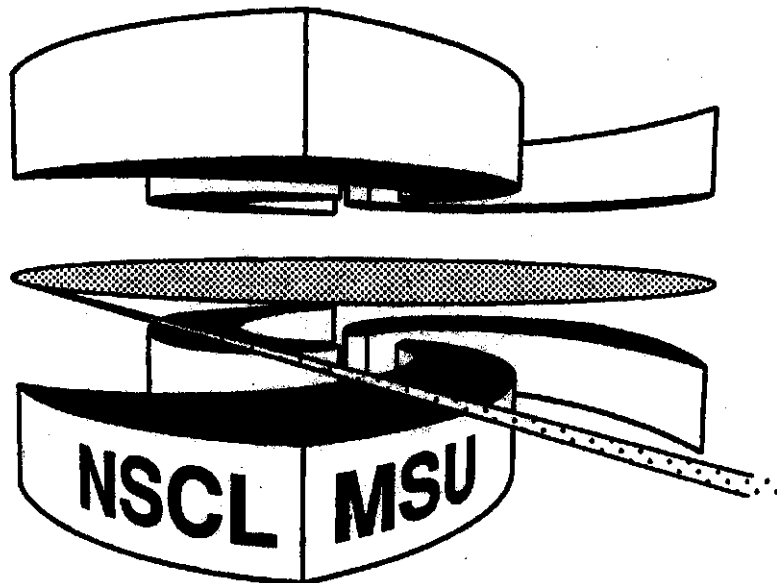


Michigan State University

National Superconducting Cyclotron Laboratory

**NUCLEAR FLOW IN CONSISTENT BOLTZMANN  
ALGORITHM MODELS**

**G. KORTEMAYER, F. DAFFIN, and W. BAUER**



MSUCL-997

NOVEMBER 1995

# Nuclear Flow in Consistent Boltzmann Algorithm Models

G. Kortemeyer, F. Daffin, and W. Bauer

*NSCL/Cyclotron Laboratory*, Michigan State University, East Lansing, MI  
48824-1321, U.S.A.

---

## Abstract

We investigate the stochastic Direct Simulation Monte Carlo method (DSMC) for numerically solving the collision-term in heavy-ion transport theories of the Boltzmann-Uehling-Uhlenbeck (BUU) type. The first major modification we consider is changes in the collision rates due to excluded volume and shadowing/screening effects (Enskog theory). The second effect studied by us is the inclusion of an additional advection term. These modifications ensure a non-vanishing second virial and change the equation of state for the scattering process from that of an ideal gas to that of a hard-sphere gas. We analyse the effect of these modifications on the calculated value of directed nuclear collective flow in heavy ion collisions, and find that the flow slightly increases.

---

## 1 Introduction

One of the still most challenging questions in nuclear physics is that of the equation of state (EOS) of nuclear matter [1]. To investigate the properties of nuclear matter at high densities and temperatures, heavy ion collisions are of great importance, and various experiments are conducted for that purpose. The simulation of such collisions however is equivalent to solving a quantum-mechanical many-body problem, which to date is not fully possible. Different approaches have been made to nevertheless approximate the solution. One method is that of Molecular Dynamics (see for example [2]), in this method both the long-range attractive (soft) and the short-range repulsive (hard) part of the particle interaction is parametrized by potentials, the trajectories are continuously updated in response to the local potential.

Another semi-classical particle-based method is the BUU approach. Here the soft part of the interaction is represented by mean fields, while the hard part is given by an explicit collision term. The collision term itself can again be

represented in different ways, especially the criteria for a collision to happen are model dependent. In many codes, this decision is based on geometrical considerations, for example, a collision is generated at the point of closest approach between two particles (see for example [3,4]).

One particular implementation of the collision term in BUU codes is the Direct Simulation Monte Carlo approach (DSMC), see for example Lang. et al. [5], and Danielewicz [6]. In this approach, collisions are not generated through geometrical and particle-trajectory based criteria, but stochastically in a way that the correct collision rate is reproduced. In a collision only momenta and energy of the particles are changed, while the particles themselves stay in place until the next advection step – the particles are assumed to be pointlike.

It was suggested that in order to reproduce a Hard-Sphere Boltzmann Equation, the DSMC approach should be extended by an additional advection that should take place after any collision [7], and by a modification the collision probability itself [7,8]. This advection is supposed to push the collision partners away from each other according to their hard-sphere radius, and the collision probability is adjusted to take into account the excluded volume of the hard spheres and screening effects. The modified DSMC method is called Consistent Boltzmann Algorithm (CBA).

In this paper we study the effect of those modifications on the nuclear flow. In section 2 we describe the theoretical background of our calculations, and section 3 presents our results and conclusions.

## 2 Theoretical Background

In the DSMC approach, the positions and momenta of the particles are evolved in a two-step process, namely advection and collisions, corresponding to one timestep of the simulation. During the advection step the particles are propagated according to their momenta. During the collision step first the particles are sorted into spatial cells of volume  $V$ . Then out of the  $n$  particles within a given box, at random,  $m$  combinations are chosen and scattered with the probability

$$W = \frac{\sigma(\sqrt{s})v_{\text{rel}}\Delta t}{NV} \frac{n(n-1)/2}{m}, \quad (1)$$

where  $\sigma(\sqrt{s})$  is the energy-dependent elementary hadron-hadron cross section,  $N$  is the number of testparticles representing one nucleon in a full-ensemble testparticle algorithm [9],  $\Delta t$  is the timestep length, and  $v_{\text{rel}}$  is the relative velocity of the particle pair [5]. In the limit  $V \rightarrow 0$ ,  $\Delta t \rightarrow 0$ ,  $N \rightarrow \infty$ , the

solutions of this method have been shown to converge to the exact solution of the Boltzmann equation [10].

This approach does not take into account the finite size of the nucleons; the testparticles are point-like, and if it was not for the contribution of the mean field, they would be following an ideal gas equation of state. It has therefore been suggested by Alexander et al. [7] to include an extra displacement  $\mathbf{d}$  of the collisions partners,

$$\mathbf{d} = \frac{1}{2} \frac{\mathbf{v}'_r - \mathbf{v}_r}{|\mathbf{v}'_r - \mathbf{v}_r|} \sqrt{\frac{\sigma(\sqrt{s})}{\pi}}, \quad (2)$$

$\mathbf{v}_r = \mathbf{v}_1 - \mathbf{v}_2$  being the velocity difference before, and  $\mathbf{v}'_r = \mathbf{v}'_1 - \mathbf{v}'_2$  being the velocity difference after the collision. Particle 1 is displaced by  $\mathbf{d}$  and particle 2 by  $-\mathbf{d}$ . This additional advection pushes the nucleons apart according to their hard-sphere radius. It is not obvious right away how this displacement scales with  $N$ . However, as in the mean free path  $1/((\sigma/N)(N\rho))$  of a testparticle,  $\rho$  being the nuclear density, there is no  $N$  dependence, the average number of collisions that a certain testparticle is involved in is independent of  $N$ . Therefore, in order to achieve the same total displacement during the course of the simulation, the individual displacement per collision should not depend on  $N$  either. The testparticles are therefore pushed apart according to the nucleonic radius, and not according to the effective testparticle radius.

The finite radius of the particles also makes it impossible for one particle to be within the “spheres of influence” of the others, and thereby from the available volume  $V$  a fraction

$$\frac{n}{N} \cdot \frac{4}{3}\pi a^3 = V\rho \cdot \frac{4}{3}\pi a^3 \quad (3)$$

is occupied, where  $a$  is the average radius of the “sphere of influence” of one nucleon, and  $n/N$  is the number of nucleons in the respective box. We obtain  $a$  by randomly picking  $n$  particle combinations for a respective box and calculating their cross sections  $\sigma_i(\sqrt{s_i})$ . The Pauli principle is approximately taken into account by only choosing particle combinations with partners that are not from the same nucleus, unless at least one of them had scattered before, and for the remaining combinations taking into account the reduced phase space volume. With  $p_B$  being the momentum of the beam per nucleon, and  $p_F$  being the Fermi momentum, we obtain for  $a$  in this approximation

$$a = \frac{1}{2} \sqrt{\frac{1}{\pi} \left( \frac{1}{n} \sum_{i=1}^n \sigma_i(\sqrt{s_i}) \right) \cdot \left( 1 - 2 \frac{p_F^3}{(p_F + p_B)^3} \right)}. \quad (4)$$

For small  $E_{\text{lab}}$ , this effective radius is about 0.84 fm, in the range between 100-400 MeV it is about 0.47 fm. This is slightly larger than what has recently

been suggested in Ref. [11], there, the effective radius derived from delays in elementary processes is about 0.6-0.8 fm and 0.15-0.3 fm, respectively.

Due to the reduced volume

$$\tilde{V} = \left(1 - \rho \cdot \frac{4}{3}\pi a^3\right) V \quad (5)$$

alone, a modified higher scattering probability

$$\tilde{W} = \frac{V}{\tilde{V}} W \quad (6)$$

has to be used. However, the scattering probability is lowered again by another effect: the particles are screening each other. A particle might not be available for scattering with another particle because there might be a third particle in between. It can be shown [8], that including this effect leads to a reduction of the scattering probability by a factor of

$$\left(1 - \rho \cdot \frac{11}{12}\pi a^3\right) . \quad (7)$$

Again, the product  $\rho \cdot a^3$  is independent of the number of testparticles per nucleon  $N$ . Including this factor, the modified scattering probability is

$$W' = Y^E W , \quad (8)$$

where

$$Y^E = \frac{1 - \rho \cdot \frac{11}{12}\pi a^3}{1 - \rho \cdot \frac{4}{3}\pi a^3} = \frac{1 - 11b^E \rho/8}{1 - 2b^E \rho} , \quad b^E = \frac{2}{3}\pi a^3 , \quad (9)$$

$b^E$  being the second virial coefficient as yielded by the Enskog Theory of the dense hard-spheres fluid [8]; see figure 1.

The implementation of the modifications makes the second virial of the hard part of the interaction non-vanishing;  $b^E$  is positive and therefore leads to an increase in pressure. This is partly compensated by the negative virial  $b^S$  that is due to the soft (mean field) part of the interaction; see for example [11]. The equation of state deviates from that of an ideal gas by both contributions, i.e.,

$$P = \rho kT \left(1 + \rho(b^E + b^S) + \dots\right) . \quad (10)$$

One should note at this point that the Enskog Theory is non-relativistic; both the advection vector  $\mathbf{d}$  and the excluded volume, therefore also  $Y^E$ , are calculated in a frame-dependent way.

Fig. 1. The scattering enhancement factor  $Y^E$  as a function of the average cross section. Shown is  $Y^E$  for  $\varrho = 1, 2, 3\rho_0$ .

### 3 Results and Conclusion

Our numerical calculation is based on the MSU BUU-code by Bauer et al. [4] which was modified from a geometrical formulation of the collision term to a stochastic formulation according to Ref. [5]. Only  $NN$  collisions were taken into account, which for the energies considered turned out to be a justified approximation. A full-ensemble and a parallel-ensemble implementation proved to have similar results; results for different systems were compared with both Refs. [4] and Ref. [12]; they were found in satisfactory agreement. An interesting side-result at this stage however was that changing the algorithm from geometrical to stochastic scattering increased the frame-of-reference dependence of the result: when running the simulation within the lab-frame we found an asymmetry in the flow which we attribute to the fact that in this frame the projectile is Lorentz-contracted and the target is not. Therefore within a spatial box inside of the overlap-zone of the two nuclei there are many more testparticles originating from the projectile than from the target, resulting in an asymmetry of the respective scattering rates. We are currently trying to overcome this problem by  $\gamma$ -dependent modifications of the scattering probabilities, however, so far with only little success. The flow-asymmetry vanishes when the calculation is performed in the c.m.-frame, which is what we did in this work. The geometry-based code did not appear to be sensitive to this asymmetry, however, Lorentz invariance certainly still is an issue [13]. Finally the full-ensemble version of the stochastic code was modified according to Ref. [7], and the scaling of the collision rate and the flow with the number of testparticles  $N$  was checked.

We simulated an (Au,Au)-collision at projectile energies of 250 and 400 MeV, and  $b = 3$  fm over a total time of 70 fm/c. The timestep length was 0.1 fm/c, the volume  $V$  was approximately 1.8 fm<sup>3</sup>, the number of testparticles per

Fig. 2. The nucleon configuration in the reaction plane at different times during the collision, shown is  $\rho(x, y = 0, z)$ . The two columns of panels on the left refer to the 250 MeV collisions, the two columns on the right to the 400 MeV collisions. Within those columns the respective panels on the left result from an unmodified simulation with point-like nucleons, the panels on the right from a hard-sphere simulation according to Ref. [7]. The difference is hardly visible, even though from the two latest panels one gets the impression that the nuclei disintegrate slightly more violently with the new algorithm.

nucleon  $N$  was 250,  $m$  in equation (1) was chosen to be  $n^2$ , and we used a soft momentum-dependent equation of state. Figure 2 shows the evolution of the configuration in the reaction plane, plotted is the nuclear density  $\rho(x, y = 0, z)$ .

The result for the unmodified algorithm is shown on the left, the result for the modified algorithm on the right, respectively. As expected, the nuclei dis-

Fig. 3. Collision rate for a 250 and 400 MeV (Au,Au) collision with  $b = 3$  fm versus time. The solid curve refers to the unmodified simulation, the dashed curve to the modified one. For the 250 MeV collision two dotted lines were added, the upper line refers to a calculation where only the scattering enhancement was taken into account, the lower line to a calculation that only incorporated the additional advection.

integrate slightly more violently due to the additional advection, resulting in a lower nuclear density. A calculation with the additional advection alone revealed that therefore also the collision rate decreases. However, this is partly compensated by the modified scattering probability Eq. (9). On the other hand, a calculation with the modified scattering probability alone shows a strongly enhanced collision rate, as expected. The upper panel of figure 3 illustrates this for the 250 MeV collision, the lower panel shows the collision rates for the 400 MeV collision.

Figure 4 shows the average final transverse momentum versus the reduced rapidity as an indicator for nuclear flow. From the slope at zero transverse momentum one concludes that in this specific simulation the flow increases by approximately 16% for the 250 MeV collision, and 5% for the 400 MeV collision, with the introduction of the new algorithm. Introducing only the additional advection, as already pointed out, the collision rate slightly decreases, however, the nuclear flow increases by about 8% for the 250 MeV collision. With the introduction of the modified scattering probability alone, the flow increases by about 13%. The fact that the contributions from both modifications do not “add up” indicates that a perturbative approach to their representation would not be justified.

An impact parameter averaged analysis for 250 MeV collisions with  $b \leq 5$  fm resulted in approximately 132 MeV/( $c$ -Unit of Reduced Rapidity) nuclear flow for the unmodified, and 148 MeV/( $c$ -Unit of Reduced Rapidity) for the modified algorithm (12% increase). The Plastic Ball data indicate approxi-



Fig. 4. Average final transverse momentum versus reduced rapidity of the protons in a 250 MeV (upper panel) and 400 MeV (lower panel) (Au,Au) collision with  $b = 3$  fm. The reduced rapidity is the rapidity  $Y_{\text{cm}}$  divided by the rapidity of the beam, which for the 250 MeV collision is approximately 0.36, and for the 400 MeV collision approximately 0.45. From the slope of a linear fit around the origin, one can determine the nuclear flow. The circles and the solid fit refer to the unmodified, the stars and the dashed fit to the modified algorithm. For the 250 MeV collision, the flow is  $\approx 147$  MeV/( $c$ -Unit of Red. Rap.) for the unmodified, and  $\approx 170$  MeV/( $c$ -Unit of Red. Rap.) for the modified algorithm. A calculation that only took into account the scattering enhancement resulted in  $\approx 166$  MeV/( $c$ -Unit of Red. Rap.), a calculation that only incorporated the additional advection in  $\approx 159$  MeV/( $c$ -Unit of Red. Rap.). For the 400 MeV collision, the flow for the unmodified algorithm is  $\approx 185$  MeV/( $c$ -Unit of Red. Rap.); for the modified algorithm it is  $\approx 195$  MeV/( $c$ -Unit of Red. Rap.).

mately 130 MeV/( $c$ -Unit of Red. Rap.) [14] nuclear flow, the EOS data only 119 MeV/( $c$ -Unit of Red. Rap.) [15]. For 400 MeV collisions the same calculations resulted in approximately 166 MeV/( $c$ -Unit of Red. Rap.) nuclear flow for the unmodified, and 185 MeV/( $c$ -Unit of Red. Rap.) for the modified algorithm (11% increase; Plastic Ball:  $\approx 169$  MeV/ ( $c$ -Unit of Red. Rap.) [14]; EOS:  $\approx 151$  MeV/( $c$ -Unit of Red. Rap.) [15]).

Overall we found the effect of the additional advection and the modified scattering probability to be significant, but not crucial. Their implementation moves the outcome of the simulations away from the experimental results. This indicates the need for an in-medium reduction of the  $NN$  cross section. This type of reduction was first found to be needed in studies of the disappearance of flow [16] and later also in theoretical studies based on thermodynamic  $T$ -matrix theory at finite temperature [17]. These results were obtained by algorithm with closest approach techniques. If one wishes to address the question of the nuclear equation of state with a DSMC algorithm, however, the corrections discussed in the present paper should be taken into account.

## Acknowledgments

We acknowledge useful discussions with P. Danielewicz. Research supported by an NSF presidential faculty fellow award and by NSF grants 9017077 and 9403666, and by the Studienstiftung des Deutschen Volkes (GK).

## References

- [1] L. P. Czernai, and J. I. Kapusta, *Phys. Rep.* **131** (1986) 223;  
S. Das Gupta, and G. D. Westfall, *Physics Today* **46**(5) (1993) 34;  
R. Stock, *Phys. Rep.* **135** (1986) 259;  
H. Gutbrod *et al*, *Rep. Prog. Phys.* **52** (1989) 1267.
- [2] J. Aichelin, *Phys. Rep.* **202** (1991) 233;  
H. Feldmeier, *Nucl. Phys.* **A515** (1990) 147;  
A. Ono *et al.*, *Prog. of Theoret. Phys.* **87** (1992) 1185;  
H. Sorge, H. Stöcker, and W. Greiner, *Nucl. Phys.* **A498** (1989) 567c;  
H. Sorge, H. Stöcker, and W. Greiner, *Ann. Phys.* **192** (1989) 266.
- [3] G. F. Bertsch, and S. Das Gupta, *Phys. Rep.* **160** (1988) 189;  
J. Aichelin, *Phys. Rev.* **C33** (1986) 537;  
H. Stöcker, and W. Greiner, *Phys. Rep.* **137** (1986) 277;  
U. Mosel, *Annu. Rev. Nucl. Part. Sci.* **41** (1991) 29;  
W. Bauer *et al.*, *Annu. Rev. Nucl. Part. Sci.* **42** (1992) 77;  
P. Schuck *et al.*, *Prog. Part. Nucl. Phys.* **22** (1989) 181;  
Y. Pang, T. Schlagel, and S. H. Kahana, *Nucl. Phys.* **A544** (1992) 435c;  
D. E. Kahana, D. Keane, Y. Pang, T. Schlagel, and S. Wang, *Phys. Rev. Lett.* **74** (1995) 4404.
- [4] W. Bauer, G. F. Bertsch, W. Cassing, and U. Mosel, *Phys. Rev.* **C34** (1986) 2127;  
W. Bauer, *Nucl. Phys.* **A471** (1987) 604;  
W. Bauer, G. F. Bertsch, and H. Schulz, *Phys. Rev. Lett.* **69** (1992) 1888.
- [5] A. Lang, H. Badovsky, W. Cassing, U. Mosel, H.-G. Reusch, and K. Weber, *J. Comp. Phys.* **106** (1993) 391.
- [6] P. Danielewicz, and G. F. Bertsch, *Nucl. Phys.* **A533** (1992) 712 (Appendix).
- [7] F. J. Alexander, A. L. Garcia, and B. J. Alder, *Phys. Rev. Lett.* **74** (1995) 5212.

- [8] P. M. Résibois, and M. De Leener, *Classical Kinetic Theory of Fluids*, p. 156 (John Wiley & Sons, New York, 1977).
- [9] G. Welke, R. Malflied, C. Grégoire, M. Prakash, and E. Suraud, *Phys. Rev. C* **40** (1989) 2611.
- [10] H. Badovsky, *Eur. J. Mech., B/Fluids* **8** (1989) 41.
- [11] P. Danielewicz, and S. Pratt, *Phys. Rev. C* **53** (1996) 249.
- [12] P. Danielewicz, *Phys. Rev. C* **51** (1995) 716.
- [13] G. Kortemeyer, W. Bauer, K. Haglin, J. Murray, and S. Pratt, *Phys. Rev. C* **52** (1995) 2714.
- [14] H. A. Gustafson *et al.* (Plastic Ball Collaboration), *Mod. Phys. Lett. A* **3** (1988) 1323.
- [15] M. D. Partlan *et al.* (EOS Collaboration), *Phys. Rev. Lett.* **75** (1995) 2100.
- [16] G. D. Westfall *et al.*, *Phys. Rev. Lett.* **71** (1993) 1986;  
D. Kakow, G. Welke, and W. Bauer, *Phys. Rev. C* **48** (1993) 1982.
- [17] T. Alm *et al.*, *Nucl. Phys. A* **587** (1995) 815.

Fig 1, Kortemeyer

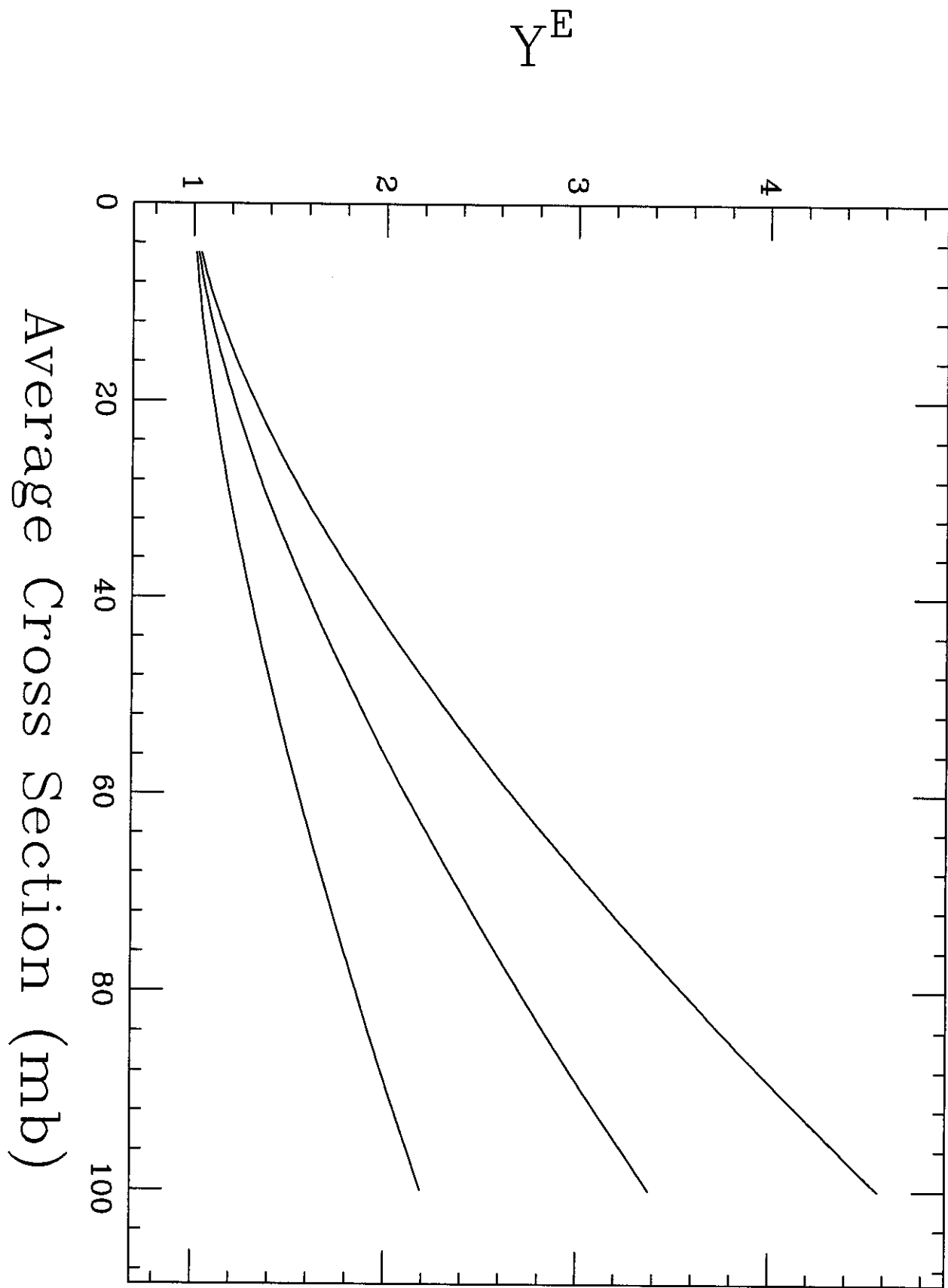


Fig 2,  
Kortemeyer

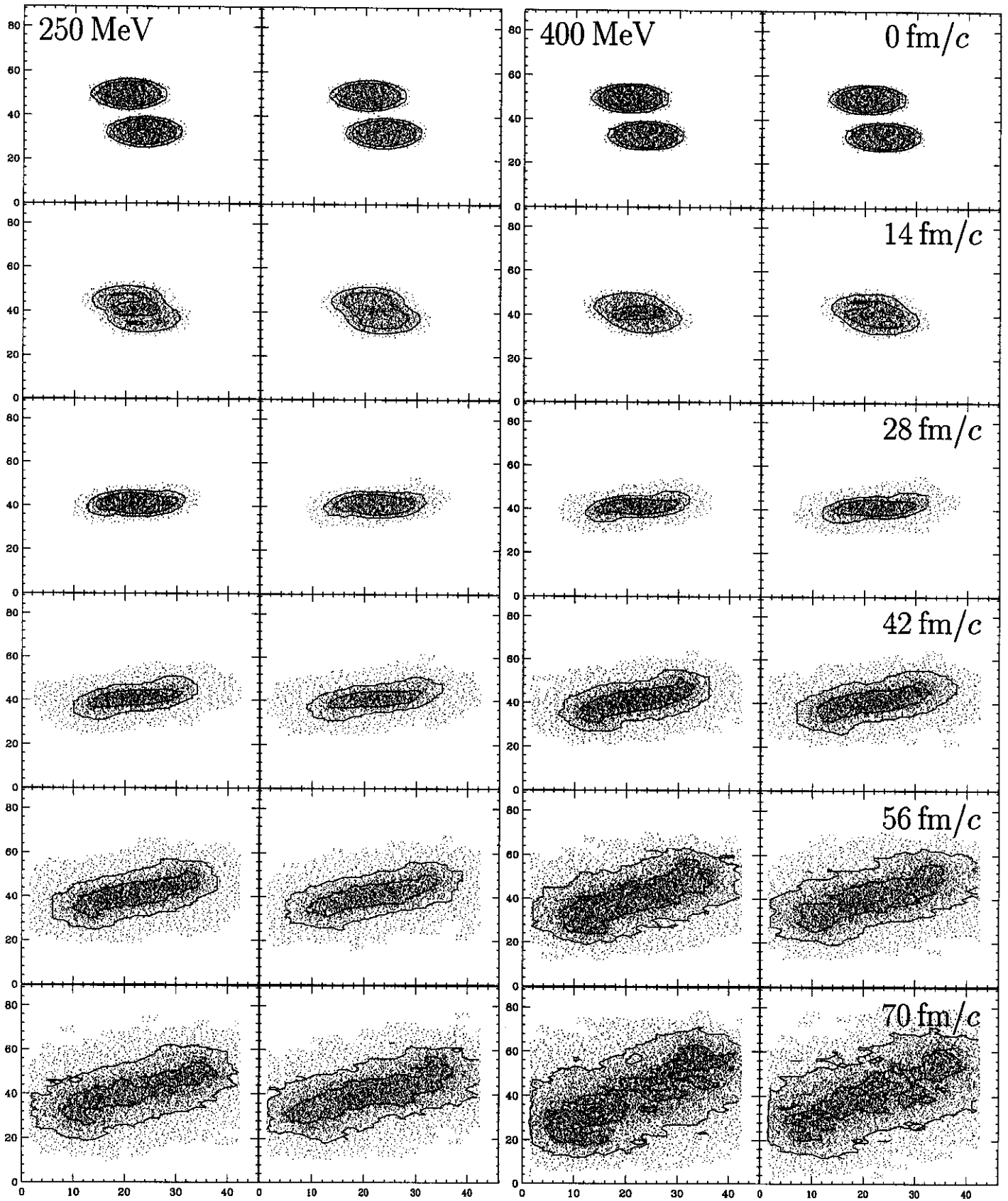


Fig 3, Kortemeyer

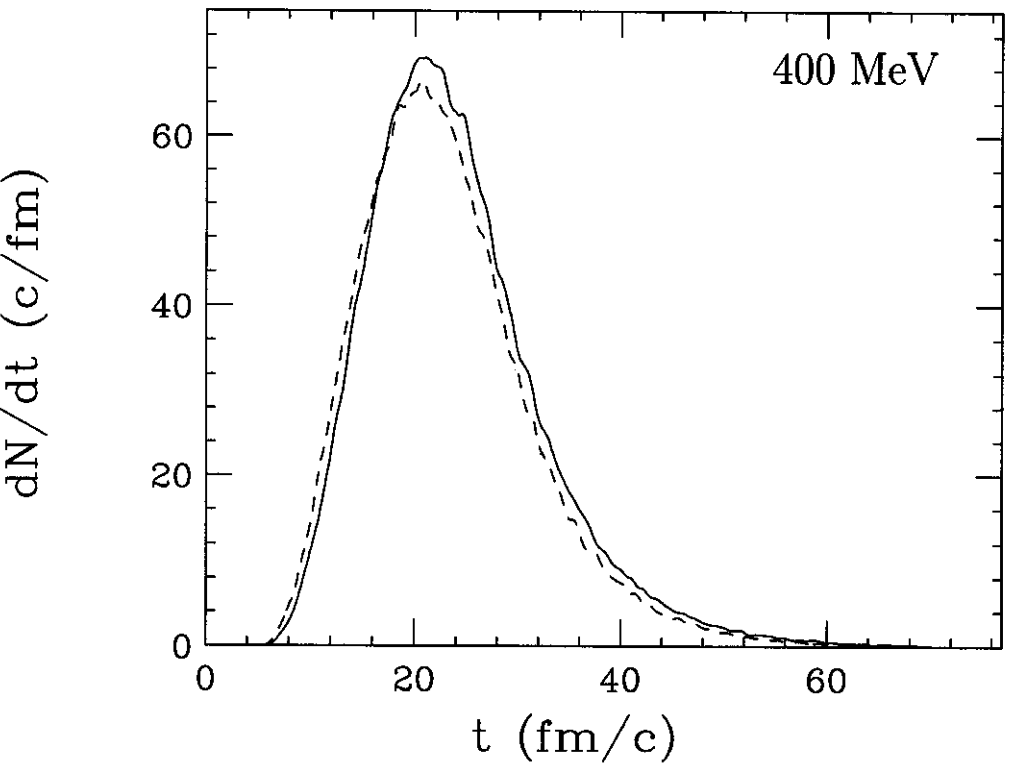
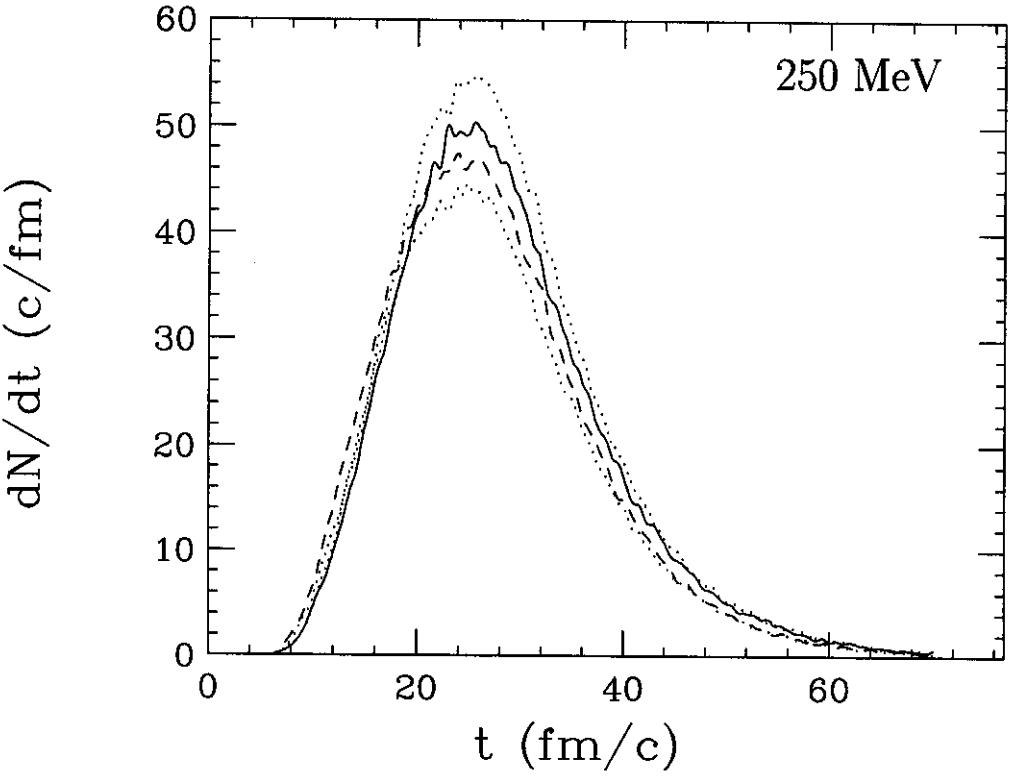


Fig 4, Kortemeyer

